

High Temperature (77–300 K) Photo- and Electroluminescence in Si/Si_{1-x}Ge_x Heterostructures

James C. STURM, Anthony St. AMOUR, Qun MI, Lori C. LENCHYSHYN¹
and Michael L. W. THEWALT¹

Department of Electrical Engineering, Photonic and Opto-Electronic Materials Center (POEM),
Princeton University, Princeton, NJ 08544 USA

¹Department of Physics, Simon Fraser University, Burnaby, BC V5A 1S6 Canada

(Received September 20, 1993; accepted for publication November 20, 1993)

The photo- and electro-luminescence of strained Si_{1-x}Ge_x/Si heterostructures on Si(100) substrates from 77 K to 300 K has been investigated both experimentally and by quantitative modelling. The key experimental features are very broad linewidths and an exponential drop in the luminescence at high temperatures, with a larger Ge fraction corresponding to a higher temperature before the drop begins. These phenomena were accurately explained by an electron-hole plasma from high carrier densities in the quantum well and by an excessively low effective lifetime in the silicon cladding region.

KEYWORDS: silicon-germanium, photoluminescence, electroluminescence, electron-hole plasma, light-emitting diode (LED), strained Si_{1-x}Ge_x/Si quantum wells

1. Introduction

Low temperature (<20 K) photo-luminescence (PL) of band-edge excitons in strained Si_{1-x}Ge_x/Si heterostructures on Si(100) substrates has now been studied by many groups.¹⁻¹² Future light-emitting devices in this material system will require an understanding of the luminescence at higher temperatures. In this paper, the photo- and electroluminescence (EL) of these structures has been investigated at temperatures up to 300 K. Models are presented to explain both the shape of the PL spectra at high temperatures and also the temperature dependence of the magnitude of the luminescence.

All samples used in this study were grown by rapid thermal chemical vapor deposition¹³ on silicon (100) substrates using dichlorosilane and germane as source gases in a hydrogen carrier. The silicon layers were grown at 700°C and the Si_{1-x}Ge_x layers at 625°C. Further growth details are in ref. 13.

2. Experimental Results

Low temperature (2–4 K) photoluminescence from Si_{1-x}Ge_x layers in strained Si_{1-x}Ge_x/Si heterostructures on Si(100) substrates has several characteristic features.¹⁻⁴ At these temperatures the luminescence is typically due to excitons bound to shallow impurities (Fig. 1). The characteristic features include a three-fold splitting of the transverse optical (TO) phonon replica due to the different Si-Si, Si-Ge, and Ge-Ge nearest neighbors, and a no-phonon (NP) recombination line which is mediated primarily by the alloy randomness and which persists to higher temperatures (>20 K) when the excitons are no longer localized. At 2 K, the linewidth of the NP line is typically on the order of 3–7 meV.

From 2 K to 77 K, there is little absolute change in the PL intensity, but there is a substantial broadening of the spectra, so that the three TO replicas are no longer distinguishable (Fig. 1). The NP peak is still clearly visible, however. In Fig. 2, the luminescence spectra

for single $x=0.2$ and $x=0.35$ Si_{1-x}Ge_x/Si quantum wells are shown for various temperatures above 77 K. The pump was a multimode green Ar⁺ laser with a power density of ~ 10 W/cm². There are two key features to note. First, the linewidths increase rapidly at high temperature. For example, while the linewidth (FWHM) of the SiGe NP line in the $x=0.2$ sample is ~ 5 meV at 2 K, it is ~ 27 meV at 77 K, and the NP peak is barely resolvable from the TO replica by 140 K. Second, the luminescence intensity decreases sharply at high temperatures, with PL from the $x=0.35$ sample persisting to higher temperatures than that for $x=0.2$. These two features will both be explained by quantitative modelling in the next two sections.

3. Electron-Hole-Plasma Effects

At temperatures sufficient to release excitons from the shallow impurity trapping sites (>20 K), free exciton luminescence should classically exhibit an $E^{1/2}e^{-E/kT}$ lineshape. However, at 77 K and higher temperatures a

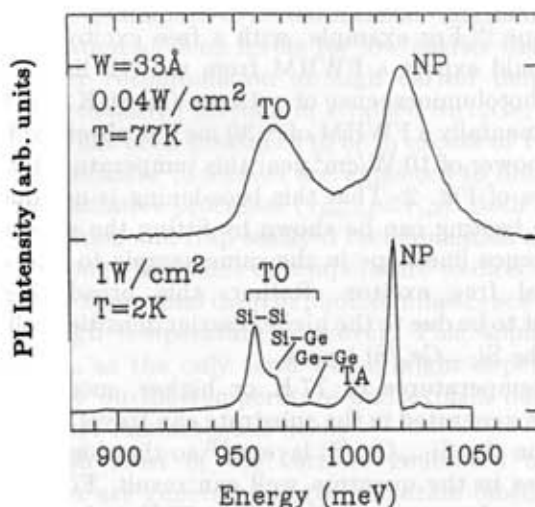


Fig. 1. 2 K and 77 K photoluminescence of ten isolated 3-nm Si/Si_{0.3}Ge_{0.2}/Si quantum wells (ref. 12).

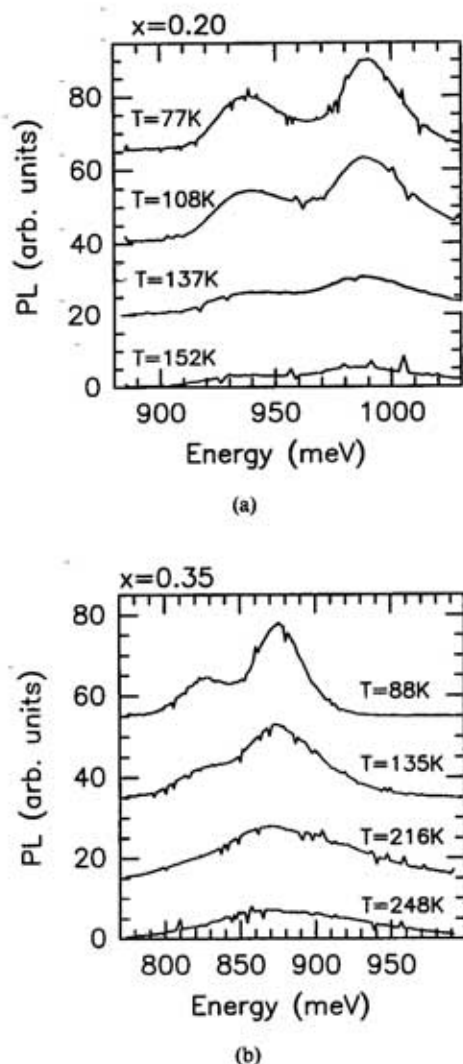


Fig. 2. Photoluminescence spectra for various temperatures of single (a) $x=0.2$ and (b) $x=0.35$ Si/Si $_{1-x}$ Ge $_x$ /Si quantum wells. (Pump power ~ 10 W/cm 2).

much broader lineshape is observed for moderate pump power levels (~ 1 W/cm 2) even when the intrinsic low temperature linewidth is included in the expected lineshape.¹⁴⁾ For example, with a free exciton model, one would expect a FWHM from the NP line in the SiGe photoluminescence of ~ 15 meV at 80 K, whereas experimentally a FWHM of ~ 30 meV is observed for a pump power of 10 W/cm 2 near this temperature for the samples of Fig. 2. That this broadening is not due to sample heating can be shown by fitting the silicon luminescence lineshape in the same sample to that of a classical free exciton. Rather, this broadening is thought to be due to the higher carrier densities collected in the Si $_{1-x}$ Ge $_x$ /Si layers.

At temperatures of 77 K or higher, most of the carriers generated in the substrate can travel to be collected in the Si $_{1-x}$ Ge $_x$ /Si layers,¹²⁾ so that high carrier densities in the quantum well can result. For carrier densities above $\sim 1 \times 10^{17}$ cm $^{-3}$ at 77 K and $\sim 5 \times 10^{17}$ cm $^{-3}$ at 300 K, the formation of an electron-hole plasma (EHP) in the Si $_{1-x}$ Ge $_x$ /Si is then favored over that

of free excitons because the carrier densities are above those for the Mott transition.¹⁴⁻¹⁶⁾ (Note this electron-hole plasma is not to be confused with the electron-hole liquid phase, sometimes seen in Si at low temperature,¹⁷⁾ which we have not observed to date.) The resulting high carrier densities push the quasi Fermi-levels into the bands so that a population inversion can easily result. A consequence of this band-filling is that the carriers participating in PL no longer need be at the band edges, with the result that a broader linewidth can result (Fig. 3). Also note that the peak PL intensity will shift to a higher energy than the fundamental bandgap.

The actual PL lineshape was modelled by starting with a low temperature spectrum $I_{LT}(E)$ to account for the intrinsic linewidth and the relative strength of the various phonon replica processes. This spectrum was then modified by first allowing the NP strength relative to the phonon replicas to vary as an adjustable parameter (taking a single value > 77 K for each sample) since the NP strength for free excitons (or an EHP) would be different than that for bound excitons, and second, adjusting the phonon replica intensities according to the expected phonon populations at elevated temperature. This modified spectrum, $I_{LT}^*(E)$, was then convoluted with all possible electron-hole transitions to yield the high temperature spectrum, $I_{HT}(E)$:

$$I_{HT}(E) = \int_0^\infty dE_n f_n(E_n) \cdot g_n(E_n) \int_0^\infty dE_p \cdot f_p(E_p) \times g_p(E_p) \cdot I_{LT}^*(E - E_n - E_p). \quad (1)$$

E_n and E_p are the electron and hole kinetic energies, g_n and g_p are the electron and hole densities of states, and f_n and f_p are the Fermi occupation functions. Although only holes are directly confined by a band offset in the Si(100)/strained Si $_{1-x}$ Ge $_x$ system, it was assumed for simplicity that Coulomb attraction would result in an equal number of electrons and holes in the Si $_{1-x}$ Ge $_x$. (The effect of the electrons on the lineshape was small compared to that of the holes in any case, however: for Si $_{1-x}$ Ge $_x$ strained on Si(100), the conduction band is four-fold degenerate at the band edge versus a single valence band, so that the hole quasi-Fermi level is much larger than the electron quasi-Fermi level for equal electron and hole densities.)

Shown in Fig. 4 are the results obtained by this

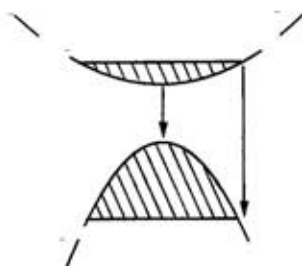


Fig. 3. Schematic diagram illustrating how band-filling effects lead to broad luminescence linewidths. A direct bandgap is illustrated only for simplicity.

model fitting photoluminescence spectra of the $x=0.35$ sample at 88 K and 216 K from Fig. 2. A carrier density of $3 \times 10^{18} \text{ cm}^{-3}$ was assumed, which, combined with the pump power of $\sim 10 \text{ W/cm}^2$ and well widths of 10 nm, corresponds to a reasonable carrier lifetime of $\sim 2 \mu\text{s}$. A very good fit is obtained in both cases, showing the suitability of the model. In Fig. 5 the above electron-hole-plasma model has been applied to the electroluminescence spectra of a p - i - n structure consisting of ten 6-nm $\text{Si}_{0.65}\text{Ge}_{0.35}$ quantum wells.¹⁸⁾ With a device area of $60 \times 60 \mu\text{m}^2$, the drive currents of 10 mA and 15 mA at cold finger temperatures of 80 K

and 300 K correspond to current densities of 280 A/cm² and 410 A/cm², respectively. Note that both the 80 K and 300 K (cold finger temperature) data could be fit very well. The TO emission from the Si cladding was not included in the model. For the two cases, fitting parameters of $T=110 \text{ K}$ and $p=n=1 \times 10^{19} \text{ cm}^{-3}$ and 350 K and $1 \times 10^{19} \text{ cm}^{-3}$ were used, respectively. That the fitted device temperatures were above the cold finger temperatures may have been caused by poor thermal contact between the cold finger and the device and an excessive power dissipation in the device due to a high series resistance.

4. Temperature Dependence

As noted earlier, between 2 K and 77 K there is little change in the integrated intensity of the PL from the $\text{Si}_{1-x}\text{Ge}_x$ (less than a factor of two change). At higher temperatures, the PL drops exponentially, with higher Ge content corresponding to a larger temperature before falling. This data of integrated PL intensity from the SiGe (including both the NP line and phonon replicas) vs temperature (and inverse temperature) is shown in Fig. 6. In this section a quantitative model for the temperature dependence of the PL is developed.

The amount of integrated PL from the SiGe depends on two factors: the fraction of the carriers generated by the pump that are collected into the SiGe (f_{SiGe}), and the ratio of the radiative and non-radiative recombination rates. The PL efficiency (η) is then

$$\eta = \frac{\tau_{\text{non-rad}}}{\tau_{\text{rad}}} \cdot f_{\text{SiGe}}, \quad (2)$$

where η is the internal PL efficiency, $\tau_{\text{non-rad}}$ is the non-radiative lifetime, and τ_{rad} is the radiative lifetime in the $\text{Si}_{1-x}\text{Ge}_x$. The radiative lifetime is due to the NP process (due to alloy scattering) and phonon-assisted transitions (predominately TO). For temperatures of 300 K or less, these rates are both expected to depend little on temperature because the phonon energies are relatively large (e.g. $\sim 58 \text{ meV}$ for the Si TO). At temperatures above 20 K, at which carriers are mobile and not localized as bound excitons or otherwise, the dominant nonradiative recombination mechanism is recombination at deep levels for low carrier densities and Auger recombination at high carrier densities. Since the radiative lifetime in strained $\text{Si}_{1-x}\text{Ge}_x$ quantum wells has been measured to be in excess of 1 ms,²⁰⁾ the non-radiative processes are expected to dominate over the radiative processes ($\tau_{\text{non-rad}} \ll \tau_{\text{rad}}$). Both Auger recombination and trap-assisted recombination are not strong enough functions of temperature to directly explain the exponential drop in photoluminescence intensity at high temperature, however. This apparently leaves f_{SiGe} as the only term which might depend exponentially on the temperature and explain our high temperature luminescence decay.

Although most of the carriers generated by the pump laser are generated in the substrate (absorption depth $\sim 1 \mu\text{m}$) and not directly in the $\text{Si}_{1-x}\text{Ge}_x$ layers, which are within the top $0.1 \mu\text{m}$ of the surface, by 77 K most of the generated carries have sufficient mobility

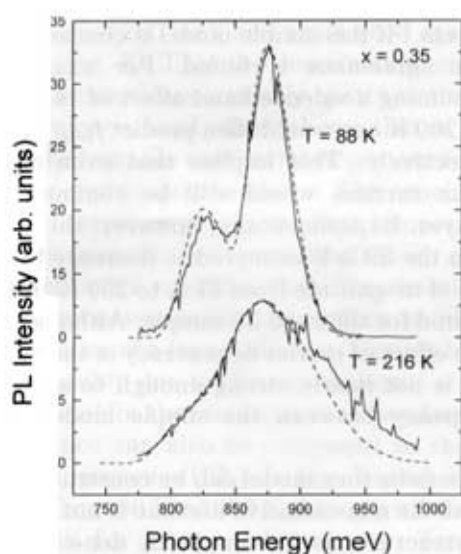


Fig. 4. Modelled photoluminescence spectra of the $x=0.35$ sample of Fig. 2 at 88 K and 216 K. A carrier density of $3 \times 10^{18} \text{ cm}^{-3}$ was used in the model.

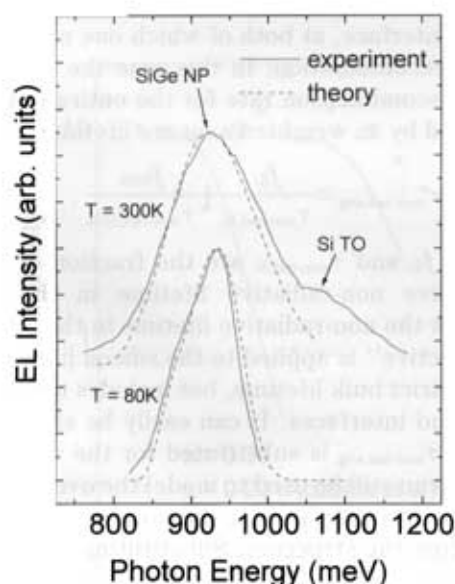


Fig. 5. Modelled and experimental (ref. 18) electroluminescence spectra of a 10 quantum well $\text{Si}/\text{Si}_{0.65}\text{Ge}_{0.35}/\text{Si}$ p - i - n structure. For a cold finger temperature of 80 K (10 mA drive current) and 300 K (15 mA drive current), the fitting parameters were temperatures of 110 K and 350 K, respectively, and a carrier density of $1 \times 10^{19} \text{ cm}^{-3}$ (both cases).

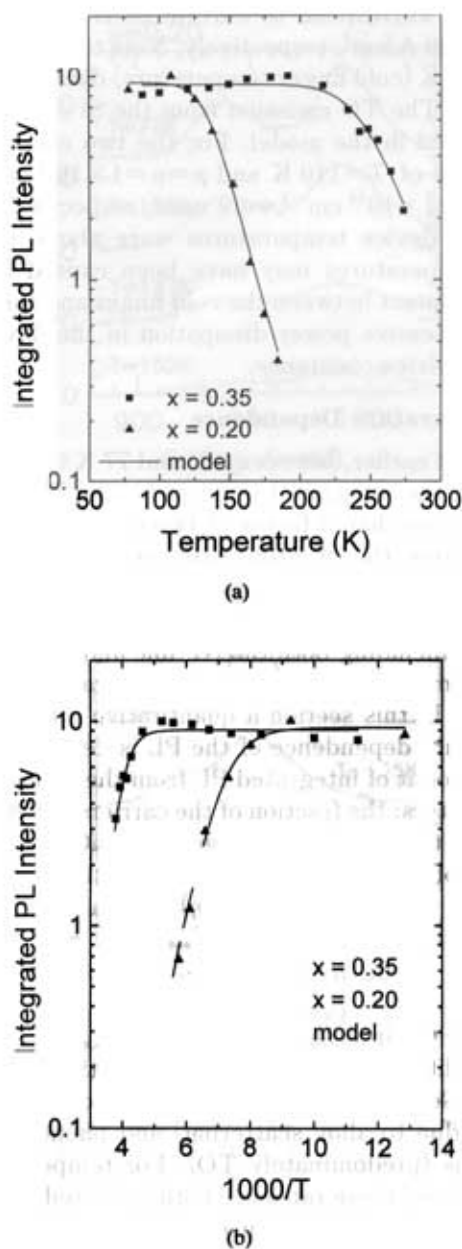


Fig. 6. Integrated SiGe photoluminescence intensity vs (a) temperature and (b) inverse temperature for the $x=0.2$ and $x=0.35$ samples of Fig. 2. The pump power was 10 W/cm^2 . The solid lines represent the model discussed in the text.

to be collected by the $\text{Si}_{1-x}\text{Ge}_x$ layer before luminescing.¹²⁾ Therefore we can assume that at temperatures over 77 K, the redistribution of carriers occurs faster than the luminescence, and that an approximate quasi-equilibrium distribution of carriers is established between the SiGe well, the capping Si layer, and over some effective distance in the Si substrate. This assumption implies that the carrier populations over these regions of interest can be described by flat quasi-Fermi levels and a thermal distribution. Furthermore, since the conduction band offset is much smaller than the valence band offset for strained $\text{Si}_{1-x}\text{Ge}_x$ on $\text{Si}(100)$,²¹⁾ the confinement effects on holes in the SiGe will be far in excess of that for electrons. Assuming holes attract electrons to yield a material that is close

to neutral in charge density so that band-bending can be neglected, the f_{SiGe} can then be expressed as:

$$f_{\text{SiGe}} = \frac{W_{\text{SiGe}}}{W_{\text{SiGe}} + W_{\text{Si}} e^{-\Delta E_v/kT}} \quad (3)$$

where W_{SiGe} is the width of the SiGe, W_{Si} is the width of the Si region over which the carriers are distributed (cap thickness plus effective width in the substrate), and ΔE_v is the valence band offset. For the samples from which the data of Fig. 6 was generated, $W_{\text{SiGe}}=10 \text{ nm}$. W_{Si} can be approximated by a minority carrier diffusion length (estimated at $\sqrt{D\tau} = \sqrt{10 \text{ cm}^2/\text{s} \cdot 10^{-6} \text{ s}} = 3 \times 10^{-3} \text{ cm}$). (The Si cap thickness of 10–20 nm does not significantly contribute to this thickness.) If this simple model is compared to the data, poor agreement is found. For example, for $x=0.2$, assuming a valence band offset of 160 meV, at 100 K and 200 K one would then predict $f_{\text{SiGe}} \sim 1.00$ and 0.91, respectively. This implies that even at 200 K 91% of the carriers would still be confined to the $\text{Si}_{1-x}\text{Ge}_x$ layer. Experimentally, however, the integrated PL from the SiGe is observed to decrease by nearly two orders of magnitude from 77 K to 200 K. A similar result is found for the $x=0.35$ sample. Although eq. (3) ignores the effect of carrier degeneracy in the $\text{Si}_{1-x}\text{Ge}_x$, this effect is not nearly strong enough to account for the discrepancy between the simple model and the data.

A more satisfactory model can be constructed by assuming that the non-radiative lifetime is not uniform in all of the structure, as was implicitly done above, but rather by assuming a substantially lower effective lifetime in the Si regions compared to the $\text{Si}_{1-x}\text{Ge}_x$ layers. If one simply considers bulk recombination, this might seem unlikely given that the SiGe was grown at a lower temperature than the Si. However, the Si region contains both the top silicon surface and the original substrate interface, at both of which one might expect excessive recombination. In this case the overall non-radiative recombination rate for the entire sample can be modelled by an weighted average lifetime, $\tau_{\text{non-rad,avg}}$:

$$\tau_{\text{non-rad,avg}}^{-1} = \frac{f_{\text{Si}}}{\tau_{\text{non-rad,Si}}} + \frac{f_{\text{SiGe}}}{\tau_{\text{non-rad,SiGe}}} \quad (4)$$

where the f_{Si} and $\tau_{\text{non-rad,Si}}$ are the fraction of carriers and effective non-radiative lifetime in the Si and $\tau_{\text{non-rad,SiGe}}$ is the non-radiative lifetime in the SiGe. The term ‘‘effective’’ is applied to the silicon lifetime since it is not a strict bulk lifetime, but includes the effects of surfaces and interfaces. It can easily be shown that if the above $\tau_{\text{non-rad,avg}}$ is substituted for the $\tau_{\text{non-rad}}$ in eq. (2), eq. (2) can still be used to model the overall SiGe luminescence intensity even if the non-radiative lifetime varies across the structure. Substituting from eq. (3)

$$\tau_{\text{non-rad,avg}} = \frac{W_{\text{SiGe}}}{\tau_{\text{non-rad,SiGe}}} \left(\frac{1 + \frac{\tau_{\text{non-rad,SiGe}} \cdot W_{\text{Si}}}{\tau_{\text{non-rad,Si}} \cdot W_{\text{SiGe}}} e^{-\Delta E_v/kT}}{W_{\text{SiGe}} + W_{\text{Si}} e^{-\Delta E_v/kT}} \right) \quad (5)$$

Combining this with eq. (2) gives a dominant temperature dependence for the PL as

$$\eta \propto \frac{1}{1 + C \cdot e^{-\Delta E_v/kT}} \quad (6)$$

where

$$C \equiv \frac{\tau_{\text{non-rad,SiGe}} \cdot W_{\text{Si}}}{\tau_{\text{non-rad,Si}} \cdot W_{\text{SiGe}}} \quad (7)$$

This expression was fit to the data of the $x=0.2$ sample in Fig. 6 using $\Delta E_v=150$ meV and $C=3 \times 10^5$, with a good agreement as shown (Fig. 6). That C is much larger than the expected $W_{\text{Si}}/W_{\text{SiGe}} \approx 30 \mu\text{m}/0.01 \mu\text{m} \approx 3000$ implies that the effective non-radiative lifetime in the Si is indeed much lower than that in the SiGe. Using a similar C (6×10^5), the $x=0.35$ data was fit using $\Delta E_v \approx 280$ meV and again good agreement was achieved (Fig. 6). That the deactivation energy for the $\text{Si}_{1-x}\text{Ge}_x$ luminescence closely matches that expected for the valence band offset shows that a large offset (and hence large Ge content) is important for obtaining high temperature luminescence. The conclusion of this section of the work is that the high temperature decay is not due to most carriers leaving the $\text{Si}_{1-x}\text{Ge}_x$ layers, but rather only a small fraction. This fraction however has a disproportionately large effect on the luminescence because of a lower effective lifetime in the silicon layers, possibly due to the top surface.

This model for the temperature dependence of photoluminescence can also be compared to the results of electroluminescence (EL). In Fig. 7, peak EL intensity is shown from 80 K to 300 K, along with the PL model predictions for integrated intensity, for the same $x=0.35$ multiple quantum well (MQW) diode described earlier in Fig. 5 at 80 K and 300 K.¹⁸ Data is also included for a similar MQW electroluminescent diode at $x=0.2$ from the work of Robbins *et al.*,¹⁹ also with model results. In both cases the EL persists to higher

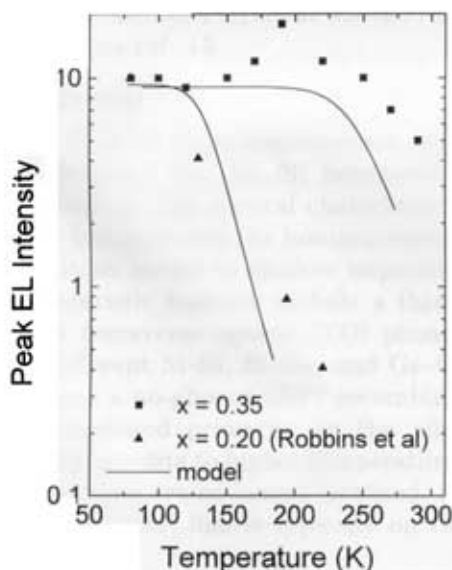


Fig. 7. Electroluminescence peak intensity vs temperature for $x=0.2$ and $x=0.35$ $\text{Si}_{1-x}\text{Ge}_x$ multiple quantum well structures, and the PL model of the text. The $x=0.2$ data is from ref. 19, and the $x=0.35$ data is from the same sample as reported at 80 K and 300 K in ref. 18.

temperature than the PL for the same composition. For example, from 100 K to 275 K the peak EL intensity for the $x=0.35$ sample changed by less than a factor of two, whereas the integrated PL decreased by a factor of five. (The origin of the feature near 200 K in the $x=0.35$ device is not understood). If the true device temperature were even higher due to internal heating effects as suggested in section 3, the discrepancy between the PL model (which accurately models the PL results) and the EL would be even more striking. A similar effect of much weaker temperature dependence of EL compared to PL has also been seen in Si/Ge short period superlattices.²² The reason for the superior performance of EL at high temperature is not known, but it appears that the decay mechanism present in PL is suppressed in the EL structures, possibly because recombination at the top surface is reduced in the p-i-n structures. Further numerical modelling and device simulation is in progress to investigate this effect.

5. Summary

In this paper the photo- and electro-luminescence from 77 K to 300 K of $\text{Si}_{1-x}\text{Ge}_x/\text{Si}$ heterostructures on Si(100) substrates has been investigated. Because of high carrier densities and resulting electron-hole plasmas, the linewidth becomes very wide at high temperatures, so that the NP line and TO replicas may already be indistinguishable by 150 K. Furthermore, at high temperatures the photoluminescence decays exponentially with temperature, with a large Ge fraction ($x \sim 0.3$) and bandgap offset from Si required for room temperature luminescence. The decrease in efficiency at high temperatures is caused by a lower non-radiative lifetime caused by increased recombination in the Si cladding layers.

The support of NSF, ONR, and NJCST for work at Princeton is gratefully appreciated. The work at Simon Fraser University was supported by the Natural Sciences Engineering Research Council of Canada.

- 1) K. Terashima, M. Tajima and T. Tatsumi: Appl. Phys. Lett. **57** (1990) 1925.
- 2) J. C. Sturm, H. Manoharan, L. C. Lenchyshyn, M. L. W. Thewalt, N. L. Rowell, J.-P. Noel and D. C. Houghton: Phys. Rev. Lett. **66** (1991) 1362.
- 3) D. J. Robbins, L. T. Canham, S. J. Barnett, A. D. Pitt and P. Calcott: J. Appl. Phys. **71** (1992) 1720.
- 4) D. Dutarte, G. Bremond, A. Souifi and T. Benyattou: Phys. Rev. B **44** (1991) 11525.
- 5) T. D. Steiner, R. L. Hengehold, Y. K. Yeo, D. J. Godbey, P. E. Thompson and G. S. Pomrenke: J. Vac. Sci. Technol. B **10** (1992) 924.
- 6) J.-P. Noel, N. L. Rowell, D. C. Houghton, A. Wang and D. D. Perovic: Appl. Phys. Lett. **61** (1992) 690.
- 7) L. Vescan, A. Hartmann, K. Schmidt, Ch. Dieker, H. Luth and J. Jager: Appl. Phys. Lett. **60** (1992) 2183.
- 8) G. A. Northrup, J. F. Morar, D. J. Wolford and J. A. Bradley: Appl. Phys. Lett. **61** (1992) 192.
- 9) S. Fukatsu, N. Usami and Y. Shiraki: Jap. J. Appl. Phys. **32** (1993) 1502.
- 10) M. Wachter, F. Schaffler, H.-J. Herzog, K. Thonke and R. Sauer: Appl. Phys. Lett. **63** (1993) 376.
- 11) X. Xiao, C. W. Liu, J. C. Sturm, L. C. Lenchyshyn, M. L. W.

- Thewalt, R. B. Gregory and P. Fejes: *Appl. Phys. Lett.* **60** (1992) 2135.
- 12) J. C. Sturm, X. Xiao, P. V. Schwartz, C. W. Liu, L. C. Lenchyshyn and M. L. W. Thewalt: *J. Vac. Sci. Technol. B* **10** (1992) 1998.
- 13) J. C. Sturm, P. V. Schwartz, E. J. Prinz and H. Manoharan: *J. Vac. Sci. Technol. B* **9** (1991) 2011.
- 14) X. Xiao, C. W. Liu, J. C. Sturm, L. C. Lenchyshyn and M. L. W. Thewalt: *Appl. Phys. Lett.* **60** (1992) 1720.
- 15) N. F. Mott: *Metal-Insulator Transitions* (Taylor & Francis, New York, 1990).
- 16) E. Cohen, M. D. Sturge, M. A. Olmstead and R. A. Logan: *Phys. Rev. B* **22** (1980) 771.
- 17) J. C. Hensel, T. G. Phillips, T. M. Rice and G. A. Thomas: *Solid State Phys.* **32** (1977) 207.
- 18) Q. Mi, X. Xiao, J. C. Sturm, L. C. Lenchyshyn and M. L. W. Thewalt: *Appl. Phys. Lett.* **60** (1992) 3177.
- 19) D. J. Robbins, P. Calcott and W. Y. Leong: *Appl. Phys. Lett.* **59** (1991) 1350.
- 20) L. C. Lenchyshyn, M. L. W. Thewalt, J. C. Sturm, P. V. Schwartz, N. L. Rowell, J.-P. Noel and D. C. Houghton: *J. Electron. Mater.* **22** (1993) 233.
- 21) C. G. Van de Walle and R. M. Martin: *Phys. Rev. B* **34** (1986) 5621.
- 22) J. Olajos, J. Engvall, H. G. Grimmeiss, E. Kasper, H. Kibbel and H. Presting: *Proc. Symp. Mater. Res. Soc.* **298** (1993).